

THE GALAXY ENVIRONMENT OF O VI ABSORPTION SYSTEMS

JOHN T. STOCKE, STEVEN V. PENTON, CHARLES W. DANFORTH, J. MICHAEL SHULL, JASON TUMLINSON,¹ AND KEVIN M. MCLIN²
 Center for Astrophysics and Space Astronomy, Department of Astrophysical and Planetary Sciences, Box 389, University of Colorado,
 Boulder, CO 80309; stocke@casa.colorado.edu, spenton@casa.colorado.edu, danforth@casa.colorado.edu,
 mshull@casa.colorado.edu, jason.tumlinson@yale.edu, mclin@universe.sonoma.edu

Received 2005 July 28; accepted 2005 December 9

ABSTRACT

We combine a *FUSE* sample of O VI absorbers ($z < 0.15$) with a database of 1.07 million galaxy redshifts to explore the relationship between absorbers and galaxy environments. All 37 absorbers with $N_{\text{O VI}} \geq 10^{13.2} \text{ cm}^{-2}$ lie within $800 h_{70}^{-1}$ kpc of the nearest galaxy, with no compelling evidence for O VI absorbers in voids. The O VI absorbers often appear to be associated with environments of individual galaxies. Gas with $10\% \pm 5\%$ solar metallicity (O VI and C III) has a median spread in distance of $350\text{--}500 h_{70}^{-1}$ kpc around L^* galaxies and $200\text{--}270 h_{70}^{-1}$ kpc around $0.1L^*$ galaxies (ranges reflect uncertain metallicities of gas undetected in Ly α absorption). In order to match the O VI line frequency, $(dN/dz) \approx 20$ for $N_{\text{O VI}} \geq 10^{13.2} \text{ cm}^{-2}$, galaxies with $L \leq 0.1L^*$ must contribute to the cross section. Ly α absorbers with $N_{\text{H I}} \geq 10^{13.2} \text{ cm}^{-2}$ cover $\sim 50\%$ of the surface area of typical galaxy filaments. Two-thirds of these show O VI and/or C III absorption, corresponding to a $33\%\text{--}50\%$ covering factor at $0.1 Z_{\odot}$ and suggesting that metals are spread to a maximum distance of $800 h_{70}^{-1}$ kpc, within typical galaxy supercluster filaments. Approximately 50% of the O VI absorbers have associated Ly α line pairs with separations $(\Delta v)_{\text{Ly}\alpha} = 50\text{--}200 \text{ km s}^{-1}$. These pairs could represent shocks at the speeds necessary to create copious O VI, located within $100 h_{70}^{-1}$ kpc of the nearest galaxy and accounting for much of the two-point correlation function of low- z Ly α forest absorbers.

Subject headings: galaxies: dwarf — galaxies: starburst — intergalactic medium — quasars: absorption lines — ultraviolet: galaxies

1. INTRODUCTION

Warm, photoionized gas in the intergalactic medium (IGM) contains virtually all the baryons in the universe at $z > 2$. With the growth of large-scale structure at later cosmic times, much of this gas cools into clumps and galaxies, while other gas is shock heated to temperatures of $10^5\text{--}10^7$ K (Cen & Ostriker 1999; Davé et al. 1999). Even at $z \sim 0$, approximately 30% of all baryons still reside in the warm ($T \approx 10^4$ K) photoionized Ly α forest (Penton et al. 2004, hereafter Paper IV). Another 30%–40% of the baryons may reside in even hotter gas ($T = 10^5\text{--}10^7$ K), the “warm-hot IGM” or WHIM (Cen & Ostriker 1999; Davé et al. 1999; Nicastro et al. 2005).

In a series of papers using moderate-resolution spectrographs aboard the *Hubble Space Telescope* (*HST*), the Colorado group has identified a sample of nearly 200 Ly α absorbers (Penton et al. 2000b, hereafter Paper I; Penton et al. 2000a, hereafter Paper II; Paper IV). The Ly α absorption line is sensitive to warm, photoionized gas, and high-sensitivity *HST* spectra with $10\text{--}20 \text{ km s}^{-1}$ resolution can detect absorbers with $N_{\text{H I}} \geq 10^{12.5} \text{ cm}^{-2}$. Hotter, shock-heated gas is less easily detected because the Lyman lines become weak and broad with increasing temperatures, while higher ionization metal lines (C III, C IV, O VI, Ne VIII) require gas of significant metallicity ($\geq 3\%$ solar metallicity) in order to be detectable.

The search for the WHIM has now begun, both in the soft X-rays and with the sensitive ultraviolet O VI resonance lines at $z \geq 0.12$ with the Space Telescope Imaging Spectrograph (STIS) on *HST* (Tripp et al. 2000, 2006; Savage et al. 2002) and at $z \leq 0.15$ with the *Far Ultraviolet Spectroscopic Explorer* (*FUSE*)

as described by Danforth & Shull (2005, hereafter DS05). At the present time, the *HST* and *FUSE* approaches have each netted ~ 40 O VI absorbers. An analysis (DS05) of the absorber frequency per unit redshift suggests that $\sim 5\%$ of all local baryonic mass is in WHIM at $10^5\text{--}10^6$ K, assuming that 20% of the oxygen is in O VI and that $[\text{O}/\text{H}] \approx -1$. This baryon assessment assumes that all O VI absorbers are formed in collisionally ionized gas (Danforth & Shull 2005; Savage et al. 2005), although photoionization models can reproduce some of the observed line strengths, widths, and ratios (Tripp et al. 2001). For a few O VI absorbers, photoionization of gas with very low density ($\sim 10^{-5} \text{ cm}^{-3}$) and large sizes (~ 1 Mpc) can provide a match to the observables (Prochaska et al. 2004; Savage et al. 2002; Tripp et al. 2001). Thus, while the O VI systems account for $\sim 5\%$ of baryons, not all of them are necessarily at temperatures identified as WHIM ($10^5\text{--}10^7$ K). The hotter WHIM is detectable only through weak X-ray absorption lines from highly ionized species such as O VII, O VIII, N VI, and N VII (Nicastro et al. 2005) or possibly very broad Ly α lines. The O VII X-ray detections are still too few to establish an accurate line density and baryon fraction, although it could be as large as suggested by simulations (Cen & Ostriker 1999; Davé et al. 1999, 2001).

The simulations have proven fairly accurate in predicting the baryon content of the warm, photoionized IGM. Some 30% of all baryons were predicted by Davé et al. (1999) to be in the 10^4 K phase at $z = 0$, and $29\% \pm 4\%$ of the baryons have been accounted for in the low- z Ly α forest surveys (Paper IV). Simulations also predict that 30%–40% of all baryons should reside in WHIM gas at the present epoch (Davé et al. 2001). An important factor in verifying this prediction is WHIM detectability. Since highly ionized metal lines are its most sensitive tracers, metallicity becomes a threshold factor. Viel et al. (2005) use numerical simulations to show that when the overdensity in dark matter and/or galaxies exceeds $\delta \geq 10$, a mean metallicity above 10% solar is

¹ Now at Department of Astronomy, Yale University, P.O. Box 208101, New Haven, CT 06520-8101.

² Now at Department of Physics and Astronomy, Sonoma State University, 1801 East Cotati Avenue, Rohnert Park, CA 94928.

expected in the IGM. Naturally, this result depends on the strength of galactic winds and their ability to spread metal-enriched gas into their surroundings. Mechanical and chemical feedback from galaxies may be more important for the WHIM than for warm, photoionized gas. Scenarios for producing O VI include outflowing winds from galaxies impacting IGM clouds or pristine IGM clouds falling into galaxies or galaxy groups (Shull et al. 2003; Tumlinson et al. 2005). Numerical simulations place WHIM gas closer to galaxies ($50\text{--}500 h_{70}^{-1}$ kpc) than the bulk of the warm, photoionized gas at $300\text{--}3000 h_{70}^{-1}$ kpc (Davé et al. 1999).

Low- z galaxy surveys along sight lines where Ly α absorption lines were detected by *HST* have been conducted by several teams (Morris et al. 1993; Lanzetta et al. 1995; Chen et al. 1998, 2000, 2005; Aracil et al. 2002; Prochaska et al. 2004; Tripp et al. 1998; Impey et al. 1999; Penton et al. 2002, hereafter Paper III) and have generally confirmed predictions for absorber-galaxy associations. In Paper III we used 46 Ly α absorbers in regions surveyed at least to L^* galaxy depths to find that the median distance from an Ly α absorber to the nearest galaxy is $500 h_{70}^{-1}$ kpc. Some absorbers were found within $100 h_{70}^{-1}$ kpc of galaxies, while others were several megaparsecs away in galaxy voids (McLin et al. 2002). Our latest sample of 138 low-redshift Ly α forest absorbers in regions well surveyed for galaxies finds that the stronger Ly α forest lines ($N_{\text{H I}} \geq 10^{13.2} \text{ cm}^{-2}$) are more tightly correlated with galaxies (Paper IV; Stocke et al. 2006) than are weaker absorbers. A recent paper by Chen et al. (2005) confirms this result, using data on the PKS 0405–123 sight line. The absorbers also cluster more strongly with each other, as confirmed by the two-point correlation function (TPCF) of low- z Ly α absorption lines (Paper IV). Simulations by Davé et al. (1999) predict that the WHIM can produce Ly α absorption with $N_{\text{H I}} \geq 10^{13.2} \text{ cm}^{-2}$, with significantly smaller nearest galaxy distances than for diffuse, photoionized gas.

In this paper we investigate the relationship between galaxies and the O VI-absorbing clouds, at the low-temperature end of the WHIM. We use the DS05 sample of 40 O VI absorbers discovered by *FUSE* (see also Danforth et al. 2006), which is currently the best sample to investigate the relationship between the WHIM and galaxies. At $z \leq 0.15$, wide-field surveys for relatively bright galaxies (limiting m_B of 16.5–19.5) can be used to search for absorber- L^* galaxy pairs out to $z_{\text{max}} = 0.04\text{--}0.15$. The deepest versions of current galaxy surveys are well matched to the sample of DS05.

In § 2 we briefly describe the O VI absorber sample and the galaxy redshift surveys used to define the relationship between O VI and galaxies. In § 3 we describe the results of this correlation study and compare the galaxy environment of O VI absorbers to Ly α absorbers in general. We also discuss a subset of O VI absorbers, whose associated Ly α lines are paired with another Ly α line at $(\Delta v)_{\text{Ly}\alpha} \leq 200 \text{ km s}^{-1}$. These O VI absorbers in Ly α line pairs are the best candidates for collisionally ionized WHIM. In § 4 we discuss our results and place the O VI absorbers into the context of galaxies, feedback/infall models, and the spread of metals into the IGM. Section 5 summarizes our most important conclusions.

2. ABSORBER AND GALAXY SAMPLES

The O VI absorber sample is described in DS05 and in more detail in Danforth et al. (2006). *FUSE* spectra were searched for O VI doublet absorptions at the redshifts of strong Ly α absorbers ($W_\lambda \geq 80 \text{ mÅ}$; $N_{\text{H I}} \geq 10^{13.2} \text{ cm}^{-2}$) found in *HST* GHRS or STIS spectra. Most of the Ly α absorbers were discussed in Papers I, II, and IV, augmented by STIS medium-resolution echelle (E140M) spectra of several bright targets observed by other investigators. Echelle sight lines were included when high-quality *FUSE* data

are available for the same targets. DS05 used *FUSE* spectra of 31 active galactic nucleus (AGN) targets to search for O VI absorption associated with 129 known Ly α absorbers with $W_\lambda \geq 80 \text{ mÅ}$. Of their 40 detections of O VI at $\geq 4 \sigma$ level, we use only the 37 detections with $N_{\text{O VI}} \geq 10^{13.2} \text{ cm}^{-2}$ for our O VI-detected sample, to ensure 90% completeness.

Our detections in $N_{\text{O VI}}/N_{\text{H I}}$ and $N_{\text{C III}}/N_{\text{H I}}$ correspond to (O/H) and (C/H) abundances of $\sim 9\%$ and $\sim 12\%$ solar, respectively. The O VI metallicity estimate is a median value for this sample as derived by DS05. It assumes an O VI ionization fraction $f_{\text{O VI}} = 0.2$ and has an estimated factor of 2 uncertainty for individual absorbers. Similar values have been obtained for individual absorbers by Prochaska et al. (2004). We therefore take 10% solar metallicity as a characteristic value for this absorber population. The O VI nondetection sample includes only those 45 absorbers (Danforth et al. 2006) with 4σ upper limits at $N_{\text{O VI}} \leq 10^{13.2} \text{ cm}^{-2}$, so that the O VI properties of these two subsamples are disjoint. If the 82 well-observed absorbers in the DS05 sample are indicative of the parent population, approximately 45% (40/82) of all higher column density Ly α absorbers have detectable O VI absorption. Danforth et al. (2006) estimate that 55% of the Ly α absorbers at $N_{\text{H I}} \geq 10^{13.2} \text{ cm}^{-2}$ have associated C III $\lambda 977$ absorption.

Bright galaxy redshift surveys available from several groups now include positions and redshifts for over 10^6 galaxies. To assemble the final galaxy catalog, we began with 494,000 galaxies in the 2005 January 7 version of the Center for Astrophysics Redshift Survey (ZCAT; Huchra et al. 1990, 1995, 1999). To this catalog we added data from other surveys, bringing the total to 1.07 million galaxies. We made the following additions and changes:

1. Replaced the ZCAT Veron-Cetty & Veron catalog version 9 entries with the current catalog entries (ver. 11; Veron-Cetty & Veron 2003³).
2. Replaced the ZCAT Sloan Digital Sky Survey (SDSS) early data release (EDR) and data release 1 and 2 (DR1 and DR2) entries of $\sim 138,000$ galaxies (Stoughton et al. 2002; Abazajian et al. 2003, 2004) with the SDSS-DR4 catalog⁴ ($\sim 550,000$ galaxies).
3. Replaced the ZCAT Two Degree Field Galaxy Redshift Survey (2dFGRS) EDR entries ($\sim 100,000$ galaxies; Colless et al. 2001) with the 2dFGRS final data release ($\sim 250,000$ galaxies; Colless et al. 2003⁵).
4. Replaced the $\sim 17,000$ ZCAT Six Degree Field Galaxy Redshift Survey (6dFGRS) EDR entries with $\sim 65,000$ entries from 6dFGRS-DR2 with well-determined redshifts (Jones et al. 2005).

These surveys were scrutinized for duplications, and several thousand duplicates were removed before we cross-correlated absorber-galaxy locations. In addition to the wide-field surveys named above, our group has conducted pencil-beam galaxy surveys along some of these specific sight lines (McLin 2002; McLin et al. 2002), adding several hundred galaxy redshifts to our final catalog. To determine the depth along each sight line to which galaxy redshifts are available down to a given galaxy luminosity (Marzke et al. 1998), we relied on the published apparent B magnitude limits for each survey and a V/V_{max} test, since more than one survey contributes along most sight lines. We applied K -corrections from Oke & Sandage (1968), appropriate for giant elliptical galaxies. In all cases, these corrections reduced the

³ Also available via the Vizier Online Data Catalog VII/235.

⁴ See <http://www.sdss.org/dr4>.

⁵ Also available via the Vizier Online Data Catalog VII/226.

distance coverage based on the V/V_{\max} tests. The published 2DF and 6DF limiting magnitudes are $B = 19.5$ and 16.8 , respectively. The SDSS claims completeness to $r = 17.8$ for the spectroscopic survey. However, not all galaxies measured photometrically above that limit were targeted with fibers in any one field because fibers cannot be placed closer than $\sim 55''$ apart. Strauss et al. (2002) determine that the overall SDSS is over 90% complete for galaxies brighter than $r = 17.8$, with completeness reaching 99% for fields without bright or closely spaced galaxies, which represent about 10% of the main sample. A similar circumstance could be important in some 2DF fields. Several other surveys, including McLin (2002), have various magnitude limits and completeness levels depending on the specific sight line observed.

We obtain good agreement for regions with completeness to L^* or better, based on the quoted magnitude limit and the V/V_{\max} test. Absorbers were rarely found close to the L^* completeness depth, although the $cz = 36,021 \text{ km s}^{-1}$ absorber toward 3C 273 lies right at the L^* completeness limit, based on a $B = 19.0$ limit set by Morris et al. (1993) and on our V/V_{\max} test. Information about the galaxy environment around this absorber is uncertain, so to be conservative we have eliminated this single absorber from our sample. This leaves 23 O VI absorbers and 32 O VI non-detections that lie in regions surveyed at least to L^* depths. For comparison, we use the stronger half of our entire Ly α absorber sample, composed of 69 absorbers with $W_\lambda \geq 68 \text{ m}\text{\AA}$ ($N_{\text{H I}} \geq 10^{13.2} \text{ cm}^{-2}$) in regions surveyed at least to L^* depths. A smaller number of absorbers in these samples have been surveyed to $0.1L^*$ depths: O VI detections (nine), O VI upper limits (eight), Ly α stronger half-sample (20), and Ly α weaker half-sample (19).

In order to determine the three-dimensional distance between absorbers and galaxies, we assume a “retarded Hubble flow” model (Morris et al. 1993) as we have done in our previous analyses (Papers III and IV). In the current analysis, we have increased the peculiar velocity difference from ± 300 to $\pm 500 \text{ km s}^{-1}$ for which we consider the galaxy and O VI absorber to be at the same redshift distance. We made this adjustment because we have found that the O VI absorption is sometimes not at the same redshift as the associated Ly α (Shull et al. 2003; Tumlinson et al. 2005). This peculiar velocity allowance, while guided by the velocity dispersion in groups of galaxies and galaxy filaments, is somewhat arbitrary (for justifications of allowances of ± 250 – 500 km s^{-1} see Lanzetta et al. 1995; Impey et al. 1999), but it does not affect our final results.

3. O VI ABSORBER–BRIGHT GALAXY ASSOCIATIONS

In order to maximize the information available to study O VI absorber-galaxy associations, we adopt two approaches to the merged galaxy redshift database. In our first approach, we construct luminosity-limited galaxy catalogs, complete along AGN sight lines to either L^* or $0.1L^*$. We specifically exclude all fainter galaxies, even when their redshifts are known. Using the methods described in § 2, we determine the maximum distance along each sight line to which galaxy redshift data are complete; regions complete to $0.1L^*$ are a small subset of the L^* -complete regions. Because few absorbers lie in regions surveyed below $0.1L^*$, this is the lowest galaxy luminosity limit that permits a sufficient sample size to draw statistical inferences.

Our second approach uses all galaxies observed along each sight line for absorbers at distances closer than the L^* or $0.1L^*$ limits. Although galaxy catalogs are well defined with a single luminosity limit, they do not use all the available redshift information. Typically, the redshift survey data are limited in apparent magnitude along any one sight line, so that absorbers at

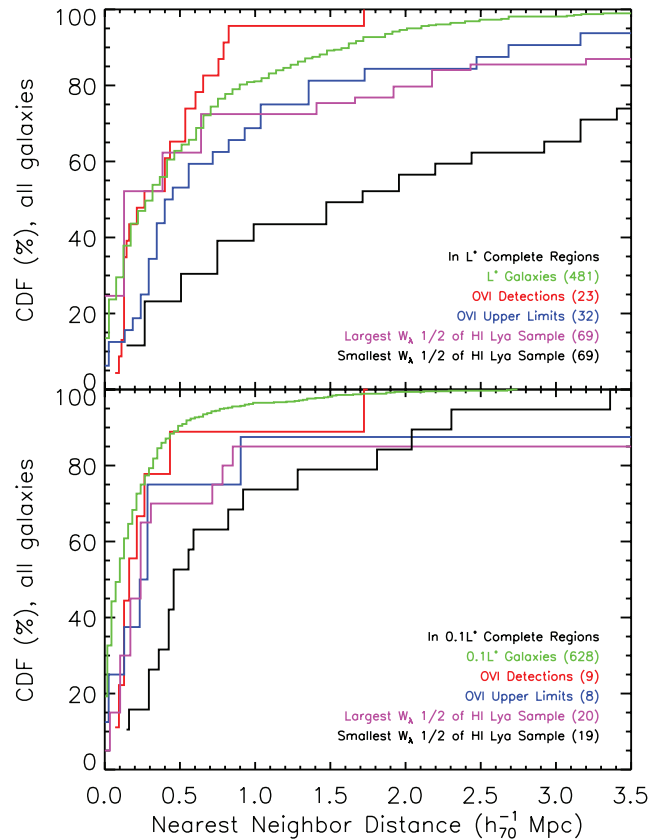


FIG. 1.—CDFs, using the all-galaxies approach of § 3, showing the distance between various types of absorbers and the nearest known galaxy in regions around absorbers, complete at least to L^* (top) and $0.1L^*$ (bottom). Also shown in green are the CDFs for the distance between galaxies in these regions.

lower redshifts are surveyed to lower galaxy luminosities. Such an approach, using an apparent magnitude–limited sample, is similar to that employed by Chen et al. (2005) to construct a galaxy-absorber cross-correlation function. The shortcoming of the second approach is that each absorber has a different luminosity completeness limit. Thus, nearest neighbor distances can be systematically smaller for very nearby absorbers because less luminous galaxies are included in the sample. In neither approach do we use absorbers in regions surveyed incompletely for galaxies. We term these two approaches as (1) “complete to L^* or $0.1L^*$ ” or (2) “all galaxies.”

Figure 1 displays the cumulative distribution function (CDF) of the nearest neighbor distances for several different samples using the all-galaxies approach. The CDFs in the top panel of Figure 1 show those absorbers in regions surveyed at least down to L^* luminosities; the bottom panel shows the $0.1L^*$ -complete regions. These CDFs are shown as the percentage of galaxies versus distance between the nearest galaxy and the following objects: (1) each galaxy at or above the limiting luminosity (green line), (2) each O VI absorber (red line), (3) Ly α absorbers with a sensitive O VI nondetection (blue line), (4) stronger Ly α absorbers from Paper IV ($W_\lambda \geq 68 \text{ m}\text{\AA}$; magenta line), and (5) weaker Ly α absorbers from Paper IV ($W_\lambda < 68 \text{ m}\text{\AA}$; black line). The O VI sample of DS05 was drawn exclusively from absorbers in the $N_{\text{H I}}$ range of the stronger half-sample [$W_\lambda(\text{Ly}\alpha) \geq 80 \text{ m}\text{\AA}$]. The sample size in each CDF is shown in parentheses. Despite the fact that this *HST*-derived sample of absorbers is at very low redshift, the number of absorbers in regions surveyed at least to $0.1L^*$ ($M_B \approx -17$) is still quite modest.

TABLE 1
MEDIAN NEAREST NEIGHBOR DISTANCES

SAMPLE (1)	L^* -COMPLETE REGIONS			$0.1L^*$ -COMPLETE REGIONS		
	$\geq L^*$	All Galaxies ^a	N^b	$\geq 0.1L^*$	All Galaxies ^c	N^b
	(h_{70}^{-1} kpc) (2)	(h_{70}^{-1} kpc) (3)	(4)	(h_{70}^{-1} kpc) (5)	(h_{70}^{-1} kpc) (6)	(7)
Galaxy-galaxy	1780	345	480	245	120	630
Ly α , stronger half ^d	1130	450	69	445	280	20
Ly α , weaker half.....	2150	1855	69	1455	480	19
O VI absorbers ^e	625	285	23	335	180	9
O VI upper limit ^e	1090	500	32	385	320	8
O VI absorbers in Ly α pairs ^e	290	190	10	^f	^f	3
C III absorbers ^e	430	150	13	^f	^f	3

^a Using all available galaxies, of any luminosity, in regions complete to at least L^* .

^b Number of galaxies or absorbers in sample.

^c Using all available galaxies, of any luminosity, in regions complete to at least $0.1L^*$.

^d $W_\lambda \geq 68$ mÅ or $\log N_{\text{HI}} \geq 13.1$ for Ly α .

^e FUSE O VI absorber sample from DS05.

^f Too few absorbers in $0.1L^*$ regions to report accurate median.

^g This sample is described in the text below.

Table 1 compares our two approaches, using the median nearest neighbor distance for samples displayed in Figure 1. If the sample size is an even number of absorbers, we report the mean of the two median numbers. Because the nearest neighbor distributions are skewed, the mean is considerably larger than the median in all cases. The mean distance between L^* galaxies in our absorber regions is $2.15 h_{70}^{-1}$ Mpc, while the median is $1.78 h_{70}^{-1}$ Mpc. The sample sizes in Table 1 are shown in columns (4) and (7).

3.1. Galaxy Statistics of Ly α Absorbers

The current Ly α absorber sample is larger than that used previously to analyze absorber environments. The CDFs in Figure 1 and the median values in Table 1 are based on 138 absorbers, compared to 46 absorbers in L^* -surveyed regions in Paper III, but our new results are consistent with those found previously. Nevertheless, it is worthwhile to revisit the basic results found in Paper III for Ly α absorbers before investigating the O VI subset. The Ly α absorbers in the stronger half-sample are more tightly correlated with galaxies than the weaker half-sample. In Table 1, the median distance to the nearest $0.1L^*$ galaxy is over 3 times larger for the weaker absorbers. Most of these absorbers lie within a few hundred kiloparsecs of a bright galaxy, a location consistent with a filament of galaxies. Yet the stronger half-sample also includes 10 Ly α absorbers ($\sim 15\%$) in galaxy voids, with nearest bright galaxy neighbors $\geq 3 h_{70}^{-1}$ Mpc away (for a justification of this limiting distance⁶ see Paper III; Drozdovsky et al. 2001).

The weaker half-sample has a CDF and median nearest galaxy distances similar to those found in numerical simulations of photoionized intergalactic gas (Davé et al. 1999). To best compare with the simulations, we use the median values in $0.1L^*$ regions for all galaxies (col. [6] in Table 1). R. Davé (2005, private

⁶ In this paper we use the terms “filament” and “void” generically to define regions where galaxies exist and those where they do not (Vogeley et al. 1991; Slezak et al. 1993), regardless of the details of the local galaxy density and its extent and shape in space. Thus, we use the term filament to refer to both spherically shaped galaxy groups and long strings of gravitationally unbound galaxies. While distances to the nearest galaxies in filament locations depend strongly on the limiting luminosities of the galaxies surveyed, this is much less true of void regions, as long as galaxies are surveyed at least down to L^* luminosities (Park et al. 2005; Hoyle et al. 2005; Szomoru et al. 1994).

communication) estimates that the Davé et al. (1999) simulations identify galaxy locations down to $0.025L^*$. The median nearest neighbor distance for simulated photoionized absorbers is $600 h_{70}^{-1}$ kpc, compared to $480 h_{70}^{-1}$ kpc observed for the weaker half-sample. This is a reasonable match, considering that the limiting galaxy luminosities of the observations and the simulations are not precisely matched and that some photoionized absorbers may be present in the stronger half-sample.

In the entire Ly α sample, $25\% \pm 4\%$ of Ly α absorbers lie in voids, more than $3 h_{70}^{-1}$ Mpc from the nearest galaxy and consistent with the $22\% \pm 8\%$ found in our smaller sample (Paper III). This fraction is also consistent with the $\sim 20\%$ of photoionized absorbers found in voids by the simulations. However, in both simulations and observations, the path lengths may not be the same through voids and superclusters. In our current sample, the relative path lengths (43% through voids, 57% through superclusters) are probably representative of the local universe, since only 4 of our 31 targets (Mrk 335, Mrk 421, Mrk 501, I Zw 1) were chosen to lie behind well-known galaxy voids. The percentage of void absorbers drops to $\sim 10\%$ for the stronger absorbers investigated for the presence of O VI absorption in this paper; this is shown in Figure 1 for both L^* and $0.1L^*$ samples.

The median distances between Ly α absorbers and L^* galaxies (Table 1) are so large ($1.1\text{--}2.2 h_{70}^{-1}$ Mpc) that it is implausible to associate all absorbers with individual L^* galaxy halos. This is because the median distance ($345 h_{70}^{-1}$ kpc) between an L^* galaxy and its nearest galaxy neighbor is a small fraction of these values, and we usually find lower luminosity galaxies between the absorber and the nearest L^* galaxy. Furthermore, the median distance between any two $\geq 0.1L^*$ galaxies ($245 h_{70}^{-1}$ kpc) is smaller than that between an absorber and its nearest $\geq L^*$ or $\geq 0.1L^*$ galaxy neighbor (625 and $335 h_{70}^{-1}$ kpc, respectively). This also makes it difficult to assign a specific galaxy at $\geq 0.1L^*$ to an individual absorber. Comparing the CDFs for the L^* -complete and $0.1L^*$ -complete samples, we find that the median nearest neighbor distances for all absorber samples scale by the expected amount if the galaxies are located randomly with respect to absorbers. For example, by extending the galaxy surveys fainter, the galaxy density is increased by an amount given by standard luminosity functions (Marzke et al. 1998; Blanton et al. 2003), and the nearest neighbor distance is decreased by approximately the cube root of that amount.

TABLE 2
GALAXIES WITHIN 200 h_{70}^{-1} kpc OF Ly α /O VI DETECTIONS

Target (1)	V_{abs}^a (km s $^{-1}$) (2)	$W(\text{Ly}\alpha)^b$ (mÅ) (3)	Galaxy Name c (4)	m_B^d (5)	M_B^e (6)	V_{gal}^f (km s $^{-1}$) (7)	Galaxy R.A. (J2000.0) (8)	Galaxy Decl. (J2000.0) (9)	D_{tot}^g (10)
3C 273	1015	369	SDSS-O587726031714779292	16.3	-14.3	903	12 28 16.0	+01 49 43.9	69
3C 273	1015	369	12285+0157	15.6	-15.4	1105	12 31 03.8	+01 40 34.2	169
H1821+643	36394	390	A1821+6420H	18.3	-20.3	36436	18 22 02.7	+64 21 38.7	162
Mrk 335	1966	220	00025+1956	16.0	-16.2	1950	00 05 29.4	+20 13 36.0	95
Mrk 876	958	324	N6140	12.6	-18.0	910	16 20 56.9	+65 23 21.7	180
Mrk 876	958	324	16224+6533	16.5	-13.9	822	16 22 49.7	+65 26 07.2	196
PG 1116+215	41579	476	A1116+2134A	18.4	-20.5	41467	11 19 06.8	+21 18 28.8	139
PG 1211+143	2130	186	I3061	14.9	-17.7	2317	12 15 04.7	+14 01 40.7	110
PG 1211+143	15384	999	McLin 396	16.7	-20.0	15242	12 14 09.6	+14 04 21.1	136
PG 1259+593	13818	685	SDSS-O587732590107885591	16.9	-19.6	13856	13 01 01.0	+59 00 06.7	138
PG 1259+593	13950	463	SDSS-O587732590107885591	16.9	-19.6	13856	13 01 01.0	+59 00 06.7	138
Ton S180	7017	222	McLin 564	19.9	-15.1	6980	00 57 04.2	-22 26 58.2	153

NOTE.—Units of right ascension are hours, minutes, and seconds, and units of declination are degrees, arcminutes, and arcseconds.

^a Heliocentric velocity (cz) of detected O VI and Ly α absorber ($N_{\text{HI}} \geq 10^{13.2}$ cm $^{-2}$).

^b Equivalent width of detected (4σ) Ly α absorber.

^c Name of nondetected galaxy. McLin indicates that the galaxy is taken from McLin et al. (2002).

^d Apparent blue (Zwicky) magnitude of galaxy.

^e Absolute blue (Zwicky) magnitude of galaxy. Our definition of an L^* galaxy is $M_B = -19.57$.

^f Heliocentric velocity (cz) of the galaxy.

^g Total Euclidean distance (in h_{70}^{-1} kpc) to the nearest absorber assuming our “500 km s $^{-1}$ retarded Hubble flow” model.

These last two statistical results are the primary evidence that low column density Ly α absorbers are not easily ascribed to individual galaxies but rather to supercluster filaments (Paper III; Stocke et al. 2006). Gas in these absorbers either is of primordial origin or comes from the cumulative debris of many galaxies in the filament. Impey et al. (1999) came to similar conclusions, using a smaller sample extending to galaxies with $M_B \leq -16$ but confined to the Virgo Cluster. Although their conclusion may be biased by the special conditions in the Virgo Cluster (see § 4), only 3 of our 31 sight lines pass through any portion of the Virgo Cluster. Assigning Ly α absorbers to supercluster filaments is also consistent with numerical simulations of the low- z Ly α forest (Davé et al. 1999). Owing to the incompleteness of the galaxy survey data at $L < 0.1L^*$, we cannot rule out the possibility that some Ly α absorbers are associated with a nearby galaxy fainter than $0.1L^*$ (see col. [6] in Table 1, Table 2, and Stocke et al. 2006).

However, DS05 found that $\sim 50\%$ of all higher column density absorbers in this Ly α absorber sample have associated O VI absorption. Thus, $\sim 25\%$ of the full sample contains metals to the detection limits of *HST* and *FUSE*. As we describe in detail in the next section, these metal-bearing absorbers may be more closely related to individual galaxies than the bulk of the low- N_{HI} IGM absorbers.

3.2. Galaxy Statistics of O VI Absorbers

Using the all-galaxies approach in Table 1 and Figure 1, we find that the median distances from an O VI absorber to the nearest galaxy in any region complete to L^* or $0.1L^*$ are comparable to the distance between galaxies in these regions. The O VI absorber CDFs in Figure 1 are the ones that either overlap the galaxy CDF or lie to the left of it. In many cases, it may be possible to associate individual O VI absorbers with individual galaxies, although many of these galaxies are likely to be fainter than $0.1L^*$ (see absolute magnitudes of nearest galaxies in Table 2). The nearest neighbor galaxy distances for O VI absorbers are about twice as large as predicted for shock-heated gas by numerical simulations. For instance, the median observed distance to

$0.1L^*$ galaxies is $180 h_{70}^{-1}$ kpc (Table 1, col. [6]) compared to $100 h_{70}^{-1}$ kpc in the simulations (Davé et al. 1999). A subset of O VI absorbers in Ly α pairs has even smaller nearest neighbor distances, which are better matched to the galaxy distances in simulations. These absorbers will be defined and discussed in the next section.

Because the O VI detections and nondetections were drawn from the stronger half of the Ly α absorber sample, it is not surprising that the CDFs in the top panel of Figure 1 for these three samples are similar. The O VI detections are found almost exclusively at distances $< 800 h_{70}^{-1}$ kpc from galaxies in L^* -complete regions and $< 400 h_{70}^{-1}$ kpc from galaxies in $0.1L^*$ regions. The one exception to this statement is a problematical case, discussed below. The median distances between O VI absorbers and the nearest $\geq L^*$ and $\geq 0.1L^*$ galaxy are 625 and 335 h_{70}^{-1} kpc, respectively (Table 1, cols. [2] and [5]). The medians provide plausible estimates for the typical distance that metals have been spread away from bright galaxies, even if the nearest bright galaxy is not the source of the metals. We refine these distances using covering factor estimates in § 4.

One-third of all O VI nondetections lie more than $1 h_{70}^{-1}$ Mpc ($800 h_{70}^{-1}$ kpc) from the nearest L^* ($0.1 L^*$) galaxy, a greater distance than any O VI detection. This result is expected because of the finite distances that metals can be spread away from galaxies in the present-day universe (Tumlinson & Fang 2005). Gas blown $1 h_{70}^{-1}$ Mpc from its source would require a mean wind speed of 500 km s $^{-1}$ acting for 2 Gyr. Outflowing winds from galaxies in the present-day universe are expected to have mean speeds substantially less than this amount (Martin 2003; Stocke et al. 2006), and 2 Gyr is much longer than the typical (10^8 yr) duration for wind activity. More distant absorbers could contain metals but be too cool to produce O VI absorption. Such an effect is expected, since warm photoionized absorbers in the simulations tend to exist farther from galaxies than the collisionally ionized WHIM (Davé et al. 1999). We propose a solution to this uncertainty in § 4.

The CDF for the O VI absorbers includes only one absorber in the DS05 O VI sample with no nearby ($< 1 h_{70}^{-1}$ Mpc) galaxy. The

TABLE 3
NONDETECTIONS AND WEAK $\text{Ly}\alpha$ DETECTIONS NEAR GALAXIES WITHIN $200 h_{70}^{-1}$ kpc OF SIGHT LINES

Target (1)	$V_{\text{abs}}^{\text{a}}$ (km s^{-1}) (2)	W^{b} ($\text{m}\text{\AA}$) (3)	Galaxy Name ^c (4)	m_B^{d} (5)	M_B^{e} (6)	$V_{\text{gal}}^{\text{f}}$ (km s^{-1}) (7)	Galaxy R.A. (J2000.0) (8)	Galaxy Decl. (J2000.0) (9)	$D_{\text{tot}}^{\text{g}}$ (10)
3C 273	<38	McLin 3	19.4	-14.0	3328	12 28 21.6	+01 56 46.8	176
Mrk 817	1933	29	SDSS-O588011219675513024	16.9	-15.1	1768	14 39 03.9	+58 47 17.2	153
Mrk 1383	8951	66	McLin 243	19.5	-16.0	9002	14 28 58.7	+01 13 08.0	160
PG 0804+761	1530	78	08050+7635	13.5	-18.2	1544	08 11 37.0	+76 25 16.6	144
PG 1211+143	<45	I3065	14.7	-16.2	1072	12 15 12.3	+14 25 57.7	116
PG 1211+143	<43	SDSS-O588017567636652218	16.3	-15.1	1305	12 14 14.4	+13 32 34.4	165
PG 1211+143	<41	I3077	15.4	-16.1	1411	12 15 56.4	+14 25 59.9	192
PKS 2005-489	2753	24	N6861E	14.5	-18.3	2531	20 11 01.2	-48 41 27.3	186

NOTE.—Units of right ascension are hours, minutes, and seconds, and units of declination are degrees, arcminutes, and arcseconds.

^a Heliocentric velocity (cz) of detected absorber; blank entry is for $\text{Ly}\alpha$ nondetections.

^b Equivalent width of detected (4σ) $\text{Ly}\alpha$ absorber or 3σ limit on detection.

^c Name of nondetected or weakly detected galaxy. McLin indicates that the galaxy is taken from McLin et al. (2002).

^d Apparent blue (Zwicky) magnitude of galaxy.

^e Absolute blue (Zwicky) magnitude of galaxy.

^f Heliocentric velocity (cz) of the galaxy.

^g Total Euclidean distance (in h_{70}^{-1} kpc) to the nearest absorber, assuming our “500 km s^{-1} retarded Hubble flow” model or, for nondetections, the distance to the sight line.

most isolated O VI absorber is the 13,068 km s^{-1} absorber toward Ton S180, located $1.7 h_{70}^{-1}$ Mpc from the nearest bright galaxy. This system is part of a complex of two $\text{Ly}\alpha$ absorption pairs (Paper IV) at velocities $cz = (12,192, 13,068)$ and $(13,515, 13,681)$ km s^{-1} . A figure showing these $\text{Ly}\alpha$ pairs is given in Shull (2002). We detect O VI in just one component of each pair, at 13,068 and 13,681 km s^{-1} . The higher redshift absorber pair has a nearest galaxy $285 h_{70}^{-1}$ kpc away at $cz = 13,798 \text{ km s}^{-1}$, a typical nearest neighbor distance for O VI detections. However, in our retarded Hubble flow model, this galaxy and another located $3.3 h_{70}^{-1}$ Mpc from the $cz = 13,068 \text{ km s}^{-1}$ absorber could be at comparable physical distances. Given the potential physical relationship between this complex of four $\text{Ly}\alpha$ absorptions, we cannot exclude the possibility that the 13,068 km s^{-1} absorber has a large peculiar velocity and is actually only $\sim 300 h_{70}^{-1}$ kpc from the same bright galaxy identified with the $cz \approx 13,000 \text{ km s}^{-1}$ absorbers.

We have found no compelling evidence for detectable O VI absorbers in voids. However, there is significant evidence that O VI absorbers lie within $70\text{--}400 h_{70}^{-1}$ kpc of a relatively bright ($M_B \leq -17$) galaxy. Table 2 lists 10 O VI absorber–galaxy pairs in the DS05 sample with total inferred distances $\leq 200 h_{70}^{-1}$ kpc. A large fraction of these close pairs involve low-luminosity galaxies, despite the fact that our galaxy survey is incomplete at $L < 0.1L^*$. This suggests that deeper galaxy surveys in regions near other O VI absorbers will find low-luminosity galaxies close to these absorbers.

3.3. Statistics of Nondetected $\text{Ly}\alpha$ Absorbers

To understand how far metals are spread from galaxies, it is insufficient to measure only the distance between absorbers and their nearest neighbor galaxy. We also do the reverse experiment, searching for $\text{Ly}\alpha$ absorbers at the same redshifts as galaxies located within $800 h_{70}^{-1}$ kpc of the sight line. For this census we use only those sight lines from Papers I and IV for which the sensitivity function is well determined. Excepting wavelengths obscured by Galactic absorption lines, the sensitivity function for $\text{Ly}\alpha$ absorption is relatively flat as a function of wavelength and column density. All *HST* spectra are of sufficient signal-to-noise ratio to detect $\text{Ly}\alpha$ absorption down to $N_{\text{H I}} = 10^{13.2} \text{ cm}^{-2}$. Some of the best spectra are able to detect $\text{Ly}\alpha$ absorption down to

$N_{\text{H I}} \approx 10^{12.5} \text{ cm}^{-2}$ (Paper IV). By searching within $800 h_{70}^{-1}$ kpc of all sight lines out to the maximum recession velocity for which L^* galaxies have been completely surveyed, we identified 16 galaxies with no accompanying $\text{Ly}\alpha$ absorption and 26 additional galaxies detected at $N_{\text{H I}} \leq 10^{13.2} \text{ cm}^{-2}$. In these same regions, we find 53 galaxies within $\pm 500 \text{ km s}^{-1}$ of an $\text{Ly}\alpha$ absorber.

Our previous accounting in § 3.1 assigned the $\text{Ly}\alpha$ absorber only to the nearest galaxy. In the current accounting, we should use only the nearest galaxy within 500 km s^{-1} as the “nondetected” galaxy. This method is equivalent to assigning the detections and nondetections to a galaxy supercluster filament, not to an individual galaxy, an interpretation supported by the data presented above. Galaxy filaments have typical thicknesses of $5\text{--}7 h_{70}^{-1}$ Mpc (estimate for the “Great Wall” by Ramella et al. 1992), so in a pure Hubble flow galaxies in a filament can be separated in recession velocity by $350\text{--}500 \text{ km s}^{-1}$. We thus identify 50 galaxy filaments (individual galaxies or groups of galaxies within 500 km s^{-1}) located $\leq 800 h_{70}^{-1}$ kpc from sight lines in L^* -complete regions. These filaments typically contain one to six galaxies within $800 h_{70}^{-1}$ kpc of the sight line. Of these 50 galaxy filaments ($\text{Ly}\alpha$ detections and nondetections), half lie within $\pm 300 \text{ km s}^{-1}$ of an $\text{Ly}\alpha$ absorber at $N_{\text{H I}} \geq 10^{13.2} \text{ cm}^{-2}$. Of the remaining half, 15 are detected at lower $N_{\text{H I}}$, 2 are possibly detected at $3\text{--}4\sigma$ significance, and 8 are not detected. Thus, we infer a 50% covering factor for gas at $N_{\text{H I}} \geq 10^{13.2} \text{ cm}^{-2}$ in galaxy filaments. Down to our $\text{Ly}\alpha$ detection limits, at least 80% of these filaments are covered, which would suggest a covering factor close to unity if more sensitive UV spectra were available. A total of 13 of the 40 filaments definitely detected in H I have multiple $\text{Ly}\alpha$ absorptions, although we have counted these $\text{Ly}\alpha$ complexes as single absorbers in this census. That is, the maximum covering factor of any one filament is 1. The CDFs for galaxies with nondetected $\text{Ly}\alpha$ absorbers are similar to those of the stronger $\text{Ly}\alpha$ absorbers, with median distances of $350\text{--}500 h_{70}^{-1}$ kpc. Since we have restricted our investigations to galaxies $\leq 800 h_{70}^{-1}$ kpc from each sight line, both of these CDFs are similar to the CDF for O VI absorbers shown in Figure 1.

In Table 3 we list those galaxies located $\leq 200 h_{70}^{-1}$ kpc from a sight line for which $\text{Ly}\alpha$ absorption is not detected, as well as weak absorbers detected at $N_{\text{H I}} < 10^{13.2} \text{ cm}^{-2}$. Three of these

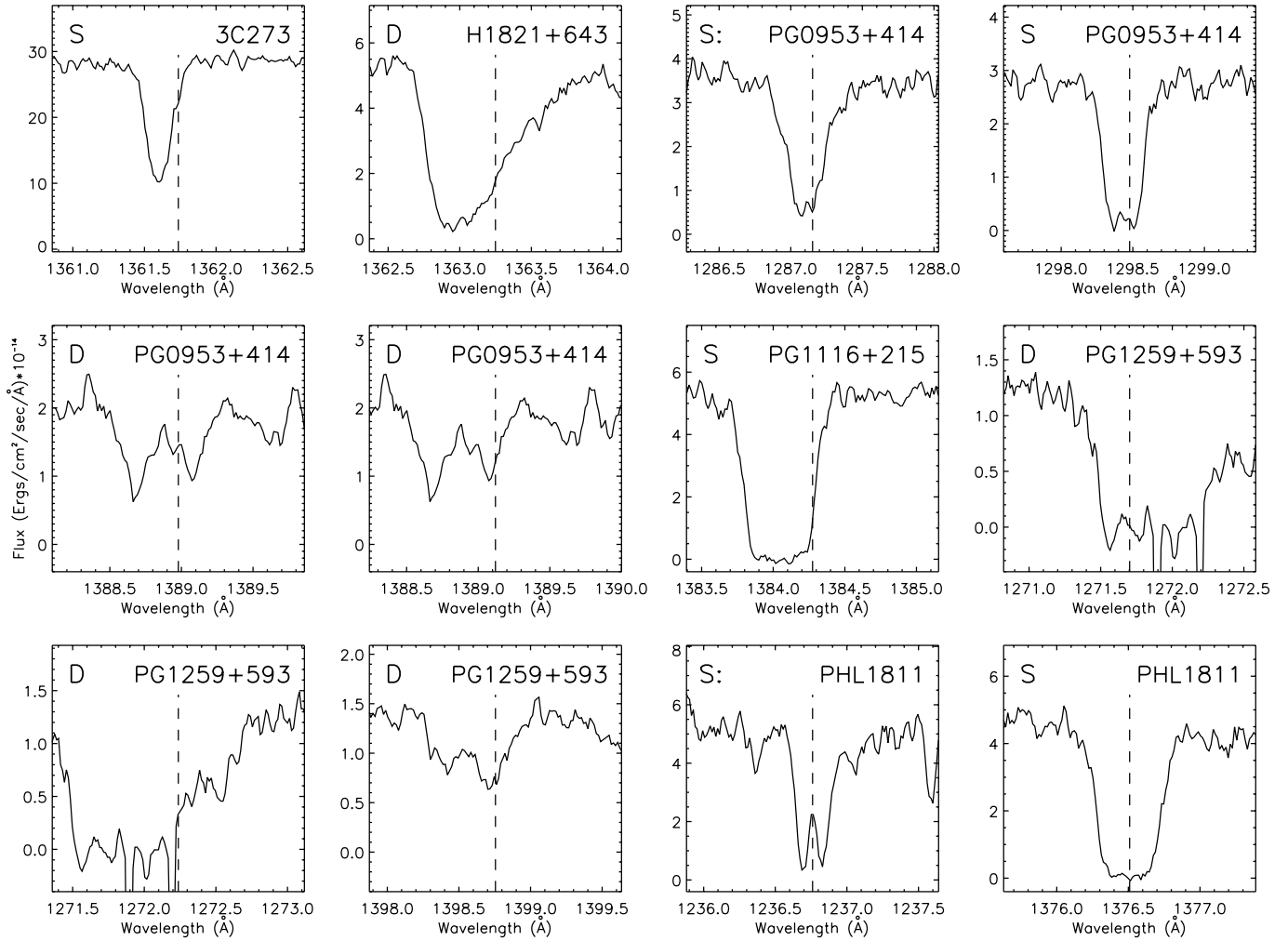


FIG. 2.—Examples of $\text{Ly}\alpha$ line profiles associated with O VI absorbers in the DS05 sample. The locations of the O VI absorption line ($\pm 0.2 \text{ \AA}$ due to errors in line centering and *FUSE* wavelength calibration) are shown as vertical dashed lines. The letter in the upper left of each panel is our proposed classification: S = single line; S: = uncertain, counted as single line; D = double line. We have classified the PHL 1811 $\text{Ly}\alpha$ line as S: despite the apparent peak in the center of the line because such a division would make each $\text{Ly}\alpha$ line implausibly narrow ($\leq 15 \text{ km s}^{-1}$).

galaxies lie near the PG 1211+143 sight line (Tumlinson et al. 2005) with recession velocities placing them in one of the Virgo Cluster “galaxy clouds.” Other Virgo galaxies, as well as a strong $\text{Ly}\alpha$ absorber, are seen at slightly higher velocities. The nondetection of the environment surrounding these galaxies may arise from special circumstances in Virgo, the only large cluster probed by this survey. The other galaxy with undetected $\text{Ly}\alpha$ absorbers lies in the 3C 273 sight line, just beyond the Virgo recession velocities. These are small numbers, but it is intriguing that three of the four galaxies within $200 h_{70}^{-1} \text{ kpc}$ of target sight lines showing no associated $\text{Ly}\alpha$ absorption lie in the Virgo Cluster, even though only 3 of our 31 sight lines pass through this cluster. Special conditions in Virgo may also explain the Impey et al. (1999) result that even very low luminosity galaxies ($M_B \leq -16$) are not obviously related to $\text{Ly}\alpha$ absorbers.

3.4. O VI in $\text{Ly}\alpha$ Line Pairs

As we pointed out in Paper IV, the excess power in the TPCF of $\text{Ly}\alpha$ absorption lines occurs exclusively within the stronger half-sample ($W_\lambda \geq 68 \text{ m\AA}$). This sample contains the O VI absorber population discussed here. Thus, we expect that some of these O VI absorbers are associated with $\text{Ly}\alpha$ absorber pairs at small velocity separations, as seen toward PKS 2155–304 (Shull

et al. 2003) and PG 1211+143 (Tumlinson et al. 2005). The GHRS and STIS spectra allow a reliable search for line pairs at $(\Delta v)_{\text{Ly}\alpha} \geq 50 \text{ km s}^{-1}$ for first-order spectra (Papers II and IV) and at $(\Delta v)_{\text{Ly}\alpha} \geq 30 \text{ km s}^{-1}$ for STIS echelle spectra. Absorbers that are blended at $\text{Ly}\alpha$ were scrutinized at $\text{Ly}\beta$ or higher Lyman lines using *FUSE* spectra. Examples of $\text{Ly}\alpha$ line profiles from the O VI absorber sample are shown in Figure 2, including single isolated lines, clear pairs of lines, complexes of more than two lines, and broad, asymmetric lines verified as pairs using higher Lyman lines. For this investigation, we group the line complexes with the line pairs, but we count each complex as only a single line pair.

The statistical results are striking: 16 of the 37 $\text{Ly}\alpha$ lines in the O VI sample are $\text{Ly}\alpha$ line pairs with $(\Delta v)_{\text{Ly}\alpha} \leq 200 \text{ km s}^{-1}$. Only some of these $\text{Ly}\alpha$ pairs show O VI absorption in both lines. Using all 21 other absorbers at $(\Delta v)_{\text{Ly}\alpha} \geq 400 \text{ km s}^{-1}$ to determine the number of close line pairs arising by chance, we expect fewer than two pairs in any $(\Delta v)_{\text{Ly}\alpha} = 200 \text{ km s}^{-1}$ interval. The presence of 16 $\text{Ly}\alpha$ absorbers in close pairs is highly significant according to the binomial probability distribution ($P_B < 10^{-10}$).

As described and listed in Papers II and IV, the TPCF excess, which is seen exclusively in the stronger half of the local $\text{Ly}\alpha$ sample (94 members), arises from 10 line pairs. We found that 11% of the stronger half-sample has $(\Delta v)_{\text{Ly}\alpha} \leq 150 \text{ km s}^{-1}$.

Within the DS05 O VI sample, we found nine Ly α line pairs (7% of the full DS05 sample) with $(\Delta v)_{\text{Ly}\alpha} \leq 150 \text{ km s}^{-1}$ and four others with $(\Delta v)_{\text{Ly}\alpha} = 150\text{--}200 \text{ km s}^{-1}$. As above, the number of Ly α lines (26) in pairs in the DS05 sample is different from the number of O VI absorbers (16) in pairs because most of the Ly α pairs do not show O VI in both lines. The two samples from Paper IV and DS05 overlap considerably, but they are not identical. Within the statistics, the O VI in Ly α line pairs can account for most of the TPCF amplitude shown in Paper IV. Using all the Ly α line pairs and complexes found in Papers II and IV, we have searched for associated O VI absorption based on our previously described limits (see § 2). In this sample we find that half are detections and half are nondetections. Thus, we suggest that O VI absorbers in Ly α line pairs may be the majority population that exhibits clustering in the low- z Ly α forest.

Ten of the 16 O VI absorbers in Ly α line pairs lie in areas surveyed for galaxies to at least L^* depth. Six of these have nearest galaxy distances $\leq 160 h_{70}^{-1}$ kpc, three have nearest galaxy distances of 200–450 h_{70}^{-1} kpc, and the last is the anomalous absorber toward Ton S180 discussed above. Despite the ambiguous circumstance of the Ton S180 absorber, the O VI in the Ly α line pairs sample is closely associated with galaxies. With a median absorber-galaxy distance of 190 h_{70}^{-1} kpc in L^* -complete regions, these absorbers lie at significantly less than the median distance between galaxies in these same regions. Just as for the O VI absorbers as a whole, the O VI absorbers with Ly α line pairs might plausibly be associated with an individual, nearby, usually faint galaxy. Unfortunately, only three O VI absorbers in Ly α line pairs are in areas surveyed for galaxies at least to $0.1L^*$ depth (see Table 1), so that an accurate assessment of the nearest faint galaxy distance is not yet possible. However, we can estimate the expected distances for $0.1L^*$ galaxies from these absorbers using the relative numbers of L^* and $0.1L^*$ galaxies present in standard luminosity functions (e.g., Marzke et al. 1998; Blanton et al. 2003). Scaling the L^* region results in Table 1 to $0.1L^*$, we expect to find fainter galaxies at a median distance of $\leq 100 h_{70}^{-1}$ kpc from these absorbers. Thus, while O VI absorbers in general have median nearest galaxy distances somewhat larger than predicted for WHIM gas by Davé et al. (1999), the O VI absorbers in Ly α line pairs match the 100 h_{70}^{-1} kpc median distance to the nearest $\geq 0.025L^*$ galaxy predicted by the simulations (Davé et al. 1999) for this IGM component.

In contrast to the O VI absorbers in Ly α line pairs, O VI absorbers associated with isolated single Ly α lines [$(\Delta v)_{\text{Ly}\alpha} \geq 400 \text{ km s}^{-1}$] have nearest neighbor distances spanning the full range shown in Figure 1 (70–800 h_{70}^{-1} kpc). Considering that some of these single lines could be unidentified pairs with velocity spacings $\leq 50 \text{ km s}^{-1}$, we estimate that $\sim 45\%$ of all O VI absorbers could be in closely spaced Ly α line pairs. Since O VI absorbers are detected in $\sim 45\%$ of all higher column density Ly α forest absorbers, this suggests that $\sim 20\%$ of Ly α absorbers with $N_{\text{H I}} = 10^{13.2}\text{--}10^{16.5} \text{ cm}^{-2}$ are members of close line pairs, at least one of which has associated O VI absorption. This population of absorbers alone accounts for $(dN/dz)_{\text{O VI}} \approx 10$ (five line pairs) per unit redshift at $z \leq 0.15$.

We have also searched for correlations of the nearest galaxy neighbor distance and the Ly α pair separation, with the “multiphase ratio,” $N_{\text{H I}}/N_{\text{O VI}}$, described in DS05. This ratio can be used to estimate the range in contributions from photoionized (H I) and collisionally ionized gas (O VI) in absorbers that appear associated kinematically. We find no correlations between the multiphase ratio and these two quantities.

The distance to the nearest neighbor galaxy is not always a reliable measure of the local environment. Therefore, we have

also searched our collective galaxy catalog for all galaxies with $|cz_{\text{abs}} - cz_{\text{gal}}| < 1000 \text{ km s}^{-1}$ within several megaparsecs of each O VI absorber. This allows us to identify nearby groups of galaxies and filamentary structures close to the absorber. The $cz \approx 17,000 \text{ km s}^{-1}$ group of four bright spiral galaxies surrounding an O VI absorber pair and associated complex of Ly α lines toward PKS 2155–304 is an obvious example (Shull et al. 2003). There are other examples, including the PG 1211+143 absorbers and galaxy group at $cz \approx 15,300 \text{ km s}^{-1}$ (Tumlinson et al. 2005) and the $cz \approx 43,000 \text{ km s}^{-1}$ O VI absorber pair in the PG 0953+415 sight line (Savage et al. 2002). Statistically, we find mixed evidence for O VI absorbers arising in groups of galaxies. Only $\sim 60\%$ (14 of 23) of the O VI absorbers lie within or near small (5–12 bright galaxies) groups of L^* galaxies, and the remainder have only one bright galaxy neighbor within 1 h_{70}^{-1} Mpc. The O VI absorbers in Ly α line pairs are no different, with only half of the sample (5/10) within or near groups of galaxies. In both small samples, the median distance from the absorber to the group centroid (defined by the nearest three galaxies to the absorber) is $\sim 250 h_{70}^{-1}$ kpc. Of course, poorer groups may be present in the other cases, but with only one galaxy brighter than L^* . Better statistics may improve these constraints.

For the present, our best assessment is that O VI absorbers, particularly those in pairs or complexes of Ly α lines, are associated with environments of individual galaxies within a few hundred kiloparsecs. These galaxies are not necessarily associated with galaxy groups. Deeper galaxy survey work in O VI absorber fields is needed to search for fainter groups.

4. IMPLICATIONS OF RESULTS

4.1. The Extent of Metal Transport

The O VI absorbers with $N_{\text{O VI}} \geq 10^{13.2} \text{ cm}^{-2}$ are associated with $\sim 45\%$ of all Ly α forest absorbers in the range $N_{\text{H I}} = 10^{13.2}\text{--}10^{16.5} \text{ cm}^{-2}$. Why are some of these H I absorbers detected in O VI and others not? No one answer may suffice. While our O VI detections are found exclusively within 800 h_{70}^{-1} kpc of the nearest galaxy in regions surveyed at least to L^* , approximately two-thirds of the O VI nondetections are found within 1 h_{70}^{-1} Mpc of the nearest galaxy in these same regions. It is reasonable to expect that Ly α absorbers at greater distances from galaxies have significantly lower metallicity, but this does not explain why many O VI nondetections have nearest neighbor distances comparable to the O VI detections.⁷

One likely possibility is that O VI-absorbing gas has less than 100% covering factor near galaxies. If this is the case, then our O VI statistics in § 3.2 overestimate the median distance to which metal-enriched gas is spread from galaxies. Another possibility is that the O VI detections and nondetections $\leq 800 h_{70}^{-1}$ kpc from galaxies have similar metallicities, whereas O VI is detected only in the most highly ionized systems, such as shocks with $(\Delta v)_{\text{Ly}\alpha} \geq 150 \text{ km s}^{-1}$. If the O VI nondetections are systematically less ionized than the detections, these absorbers will exhibit associated lower ionization metal lines, as seen in some Galactic high-velocity clouds (HVCs; Sembach et al. 1999; Collins et al. 2005). In this case, our original estimates (cols. [2] and [5] of Table 1) of median galaxy-absorber distances are accurate, and metals with $[Z] \geq -1$ have been spread to 625 ($L \geq L^*$) and 335 h_{70}^{-1} kpc ($L \geq 0.1L^*$). In these same cases, the CDFs suggest that metals

⁷ We have not yet conducted a “blind search” for O VI absorption, unassociated with Ly α absorbers. In our *FUSE* surveys, we have not found an O VI absorber without some corresponding Ly α absorption, suggesting multiphase absorbers (DS05).

TABLE 4
METAL LINE ABSORBERS

Sample Description ^a (1)	Total Number in Sample (2)	Number in L^* Regions (3)	Median NND ^b (h_{70}^{-1} kpc) (4)
O VI and C III detections.....	12	6	145
O VI detection/C III upper limit.....	8	5	540
C III detection/O VI upper limit.....	4	3	100 ^c
O VI and C III nondetections.....	21	15	1000

^a Detections and nondetections defined using column density limits $N_{C\text{III}} \geq 10^{12.6} \text{ cm}^{-2}$ and $N_{O\text{VI}} \geq 10^{13.2} \text{ cm}^{-2}$.

^b Nearest neighbor distance (NND) using the all-galaxies method, as surveyed in L^* -complete regions.

^c Note large uncertainty owing to small number statistics.

have been transported to maximum distances of 800 and 400 h_{70}^{-1} kpc, respectively.

These two hypotheses can be tested by searching for other metal absorption lines (e.g., Si II, S II, C II, Si III, C III, C IV) in *FUSE* and *HST* spectra. If the ionization threshold hypothesis is correct, we should find lower ionization states in many absorbers where O VI is not present. If this trend is driven primarily by metallicity, lower ions should be found exclusively where O VI has been found (DS05). *FUSE* spectra have detected C III $\lambda 977$ (Danforth et al. 2006) for $N_{C\text{III}} = 10^{12.6} - 10^{13.9} \text{ cm}^{-2}$. For photoionization parameters typical of low- z Ly α absorbers, *FUSE* can probe average metallicities $\sim 10\%$ solar (Danforth et al. 2006), with sensitivities down to $\sim 3\%$ solar for strong Ly α absorbers. By combining *FUSE* detections with limits on C III for photoionized gas and O VI for collisionally ionized gas, we can assess the locations of 10% solar metallicity gas in the local IGM. We know of only one low- z absorber, the 1586 km s^{-1} absorber toward 3C 273 (Tripp et al. 2002), where low-ionization metal lines are detected, but O VI and C III remain undetected. Thus, we expect that detections in either O VI and/or C III provide a nearly complete metal inventory in low column density Ly α absorbers.

Table 4 summarizes the statistics of metal detections in the DS05 sample, for $N_{O\text{VI}} \geq 10^{13.2} \text{ cm}^{-2}$ and $N_{C\text{III}} \geq 10^{12.6} \text{ cm}^{-2}$, using new results from Danforth et al. (2006). The nearest neighbor statistics differ slightly in Table 4 and Table 1. Not all O VI detections are used in Table 4 if the C III limits are poor, and not all C III detections are used if the O VI limits are poor. The samples in Table 4 are defined more precisely, but the sample sizes are much smaller (see col. [3]). Slightly over half of all Ly α absorbers with $N_{H\text{I}} = 10^{13.2} - 10^{16.5} \text{ cm}^{-2}$ have 10% solar metallicity based on *FUSE* observations of C III and O VI (DS05; Danforth et al. 2006). These statistics accurately assess both the frequency per unit redshift and the proximity to galaxies of 10% solar metallicity gas in the low- z IGM.

For the three metal-bearing absorber samples, the median distances to nearest neighbor galaxies are 100–500 h_{70}^{-1} kpc, and all three samples have maximum distances of $\sim 650 h_{70}^{-1}$ kpc from galaxies in L^* -complete regions. Using either the complete C III sample, whose nearest neighbor statistics are shown in Table 1, or the (9 of 16) C III detections in Table 4, we find that no C III metal line system lies farther than $\sim 800 h_{70}^{-1}$ kpc from the nearest bright galaxy. We conclude that low column density Ly α absorbers with nearest neighbors $>800 h_{70}^{-1}$ kpc away have $[Z] < -1$. Because there are sensitive nondetections of metals within 800 h_{70}^{-1} kpc of galaxies, regions of high metallicity cannot have a high covering factor. We can assess the galaxy proximity of the absorbers not detected in metals using the 15 O VI absorbers in L^* -complete regions from Table 4. Fully 57% of these nondetections are found $\leq 800 h_{70}^{-1}$ kpc from the nearest known galaxy. If both the metal-

rich (first three samples) and metal-poor (nondetections) absorbers in L^* -complete regions are representative, then two-thirds of the absorbers with nearest neighbor galaxies within 800 h_{70}^{-1} kpc have $\sim 10\%$ metallicity.

We can restate this result in another way. We can associate a volume extending 800 h_{70}^{-1} kpc from the nearest galaxy with the volumes within supercluster filaments of galaxies. If these galaxy filaments were filled entirely with gas with $N_{H\text{I}} \geq 10^{13} \text{ cm}^{-2}$, then metal-enriched gas ($[Z] \gtrsim -1$) has a $\frac{2}{3}$ covering factor in galaxy filaments. Neither the current absorber sample nor any other *HST*-observed sample of AGN sight lines is sufficiently dense on the sky to estimate the covering factor of a galaxy supercluster filament at a specific H I column density. Confirming the covering factor for H I gas will have to await observations of a much larger number of AGN targets in the far-UV.

Nevertheless, we can still correct for Ly α nondetections. As shown in § 3.3, only 50% of all galaxies or groups of galaxies identified as supercluster filaments are detected at $N_{H\text{I}} \geq 10^{13.2} \text{ cm}^{-2}$. The lack of a strong correlation between lower column density Ly α absorbers and galaxies (Fig. 1) and the absence of clustering of lower column density Ly α absorbers (Paper IV) suggest that weaker absorbers are not associated with galaxies and are unlikely to contain metals. Thus, we suspect that both Ly α nondetections (20% of the total) and Ly α detections at $N_{H\text{I}} < 10^{13.2} \text{ cm}^{-2}$ (30% of the total) have metallicities of $[Z] \leq -1$. On the other hand, high-temperature WHIM absorbers ($T \geq 10^6$ K) are expected to be Ly α nondetections but with observable O VII and O VIII (Fang et al. 2002; Nicastro et al. 2005). With these covering factor estimates, we decrease our best estimate for the median distance that metals are spread from L^* galaxies to 350–500 h_{70}^{-1} kpc. Around galaxies surveyed to $0.1L^*$, the corrected distance decreases to 200–270 h_{70}^{-1} kpc, even if these galaxies are not the source of the metals. The ranges indicate the uncertainty in covering factor arising from our lack of knowledge of metallicity in low- $N_{H\text{I}}$ absorbers.

Tumlinson & Fang (2005) used the observed frequency, $dN/dz = 20 \pm 3$ (DS05), of O VI absorbers with $N_{O\text{VI}} \geq 10^{13.2} \text{ cm}^{-2}$, to constrain the distribution of metals in the low- z IGM. From a large SDSS sample of galaxies and QSOs, they constructed mock catalogs of QSO/galaxy pairs. A direct association of galaxies and O VI absorbers requires a uniform (100% covering factor) metal enrichment to 750 h_{70}^{-1} kpc for $L \geq L^*$ and to 300 h_{70}^{-1} kpc for $L \geq 0.1L^*$. Danforth et al. (2006) made a similar O VI cross section calculation of 400 h_{70}^{-1} kpc ($L \geq 0.1L^*$) using the observed galaxy luminosity function (Marzke et al. 1998; Blanton et al. 2003). The difference in values obtained by these two approaches probably comes from galaxy clustering, which the Tumlinson & Fang (2005) approach automatically takes into account. If galaxies brighter than L^* (or even $0.1L^*$) were responsible for IGM

metal enrichment, we would find O VI absorbers at greater distances from these galaxies. However, a smaller number of metal production sites requires larger absorber cross sections to match the observed O VI line frequency, $(dN/dz)_{\text{O VI}}$. This requirement drives us to propose galaxies fainter than $0.1L^*$ as the primary contributors to metals in the IGM (Shull et al. 1996).

For low-luminosity galaxies to produce metal-enriched absorbers, they must disperse these metals to $\sim 100 h_{70}^{-1}$ kpc. Stocke et al. (2004) discovered one such dwarf galaxy-absorber pair in the 3C 273 sight line ($70 h_{70}^{-1}$ kpc separation on the sky), and Table 2 lists four other pairs. In general, few absorber regions have been surveyed to sufficient depth to adequately test this hypothesis. Most of the entries in Table 2 are more luminous galaxies in regions insufficiently surveyed to see whether dwarfs are present near these absorbers. Deeper searches below $0.1L^*$ are needed to uncover the other galaxies responsible for the bulk of the ~ 0.1 solar metallicity enrichment in the low- z IGM.

4.2. Amount of WHIM in O VI Absorbers

The difficulties of distinguishing O VI absorbers as collisionally ionized or photoionized have long been appreciated. In many cases, collisional ionization is favored, such as the O VI absorber at $z = 0.1212$ toward H1821+643 (Tripp et al. 2001) or the O VI and Ne VIII absorber at $z = 0.2070$ toward HE 0226–4110 (Savage et al. 2005). In other cases (Savage et al. 2002; Tripp et al. 2002; Prochaska et al. 2004) an argument can be made for photoionization. The Ly α profile of the H1821+643 absorber in Figure 2 shows absorption spread over 75 km s^{-1} . Tripp et al. (2001) suggest that this radial velocity implies a full shock velocity $\sim 130 \text{ km s}^{-1}$, within the constraints required to produce the observed O VI and H I line strengths and widths, as well as the upper limit on C IV in the case of collisional ionization.

In collisional ionization equilibrium, O VI reaches its maximum ionization fraction at $T = 10^{5.45} \text{ K}$ (Sutherland & Dopita 1993). In the nonequilibrium cooling regions behind radiative shocks, O VI forms in detectable quantities for shock velocities $V_s \geq 130 \text{ km s}^{-1}$ (Shull & McKee 1979; Indebetouw & Shull 2004), with substantial amounts produced for $V_s = 150$ – 200 km s^{-1} . The postshock temperature at an adiabatic shock front is

$$T_s = \left(\frac{3\mu V_s^2}{16k_B} \right) \approx (1.34 \times 10^5 \text{ K}) \left(\frac{V_s}{100 \text{ km s}^{-1}} \right)^2, \quad (1)$$

where $\mu \approx 0.59m_{\text{H}}$ is the mean particle mass for a fully ionized plasma with He/H = 0.08. Generalizing this result to all O VI absorbers, we expect shock-heated O VI absorbers to be members of Ly α line pairs with $(\Delta v)_{\text{Ly}\alpha} = 75$ – 150 km s^{-1} , adopting mean shock velocities $\sqrt{3}$ times the radial velocity differences. We found that a substantial fraction of O VI absorbers correspond to paired or complex Ly α absorption lines with separations $(\Delta v)_{\text{Ly}\alpha} \leq 200 \text{ km s}^{-1}$. These O VI absorbers in Ly α line pairs have nearest L^* galaxies ranging from 140 to $450 h_{70}^{-1}$ kpc, significantly less than for the full O VI sample.

This distinction of paired or nonpaired absorbers may be important, since Ly α line pairs with one or more detections of O VI are potential shock-heated absorbers. Approximately 45% of the O VI detections occur in Ly α line pairs, and O VI absorbers are seen in 45% of the higher column density Ly α absorbers. In § 3.4 we suggested that this subset (20% of the stronger Ly α absorbers) provides the best candidates for shock-heated WHIM. They typically show O VI absorption in one line of paired Ly α absorbers. A somewhat larger number is obtained using the O VI

and C III statistics in Table 4, which shows that half the metal line detections appear in both O VI and C III (Danforth et al. 2006). Other shock-heated systems may have smaller radial velocity components along the sight line. These estimates are made more difficult by the fact that many absorbers contain multiphase components of collisionally ionized and photoionized gas.

The number of O VI absorbers in Ly α line pairs is sufficient to explain the excess power in the TPCF of the low- z Ly α forest at $(\Delta v)_{\text{Ly}\alpha} \leq 200 \text{ km s}^{-1}$ (Paper IV). The O VI absorbers in Ly α line pairs also have the nearest galaxies of all the samples compiled in this paper. These distances are significantly less than for the O VI absorber sample as a whole, and they are as expected for WHIM on the basis of the numerical simulations (Davé et al. 1999). The Ly α line doubling suggests models for these WHIM absorbers involving either primordial infall onto metal-enriched galaxy halos or metal-enriched galactic winds impacting primordial IGM clouds. Because these systems involve more than one absorber, mixed ionization (multiphase) models that form both C III and O VI may naturally result. The mixed ionization and close proximity to galaxies suggest a comparison between these absorbers and the Galactic HVCs (Collins et al. 2004; Fox et al. 2005).

DS05 used the current sample of O VI absorbers to determine the WHIM contribution of the O VI absorbers to the baryon density,

$$\Omega_b(\text{O VI}) = (0.0022 \pm 0.0003) [h_{70}(Z_{\text{O}}/Z_{\odot})(f_{\text{O VI}}/0.2)]^{-1}. \quad (2)$$

This represents a baryon fraction, $\Omega_b(\text{WHIM})/\Omega_b(\text{tot}) \approx 5\%$, assuming that this gas has 10% solar metallicity and ionization fraction $f_{\text{O VI}} = 0.2$. The O VI contribution to Ω_b could be as high as 10%, considering the likely dispersion in O/H metallicity and O VI ionization fraction. Using an *HST* sample, Tripp et al. (2006) found a similar fraction of baryons (7%) in O VI absorbers at $z \geq 0.15$.

Some of the O VI absorbers may include a contribution from photoionization, which raises the issue of “double counting” in the baryon inventory (Stocke et al. 2006). In our *HST* surveys of Ly α absorbers (Papers I and IV), we converted from observed H I column densities to the total number of baryons by assuming photoionization equilibrium in warm ($\sim 10^4 \text{ K}$), mostly ionized gas. In contrast, the O VI surveys assume collisionally ionized gas at $\sim 10^{5.5} \text{ K}$. Because the H I fractions in this hot gas are low, $\sim 10^{-6}$, any Ly α absorption will be broad (FWHM $\approx 120 \text{ km s}^{-1}$) and shallow (optical depth $\tau_0 \approx 0.1$), in contrast to the observed Ly α lines, which are typically sharp and narrow ($b < 40 \text{ km s}^{-1}$). For these reasons, we believe that the Ly α surveys *do not* count H I absorption from the WHIM. One might expect a small reduction in the O VI WHIM baryon census, owing to photoionized O VI absorbers that coexist with single-phase, photoionized Ly α lines.

It is also worth elaborating on how the Ly α and O VI surveys were done. Both DS05 and Danforth et al. (2006) used the surveyed Ly α lines as “signposts” in redshift to search for corresponding O VI and C III. The fact that they found O VI in a significant fraction of cases shows that these ions are associated kinematically with the H I. Physical modeling suggests that these ions exist in a multiphase medium, in which the hot gas and warm photoionized gas share the same velocity range but are not cospatial. Such situations could arise in conductive interfaces, cooling shocks, or turbulent mixing layers. In our baryon surveys, the Ly α census counts warm photoionized baryons (30% of Ω_b) and the O VI census counts a portion of the hot (WHIM) baryons (5%–10% of Ω_b).

Our arguments in § 4.2 about shock heating suggest that O VI absorbers in Ly α pairs are collisionally ionized gas at $T = 10^5 - 10^6$ K. The other half of the O VI sample probably also includes shock-heated gas with low radial velocity components, as well as some low-density ($n_{\text{H}} \sim 10^{-5.5} \text{ cm}^{-3}$) photoionized ($T \sim 10^4$ K) gas. These absorbers would be similar to, but much more extended than, typical Ly α absorbers (for sample calculations see Tripp et al. 2001; Danforth et al. 2006). With much better statistics, one could quantify the appropriate reduction in O VI-associated baryon counts, owing to those O VI absorbers produced in single-phase (warm) photoionized gas.

5. CONCLUSIONS AND DISCUSSION

We have used the O VI sample of DS05, with 37 detections at $N_{\text{O VI}} \geq 10^{13.2} \text{ cm}^{-2}$ and 45 nondetections with upper limits below that level, to investigate the possible association of O VI absorbers with galaxies. Our sample of O VI absorbers comes from the stronger half of Ly α absorbers (Papers I and IV). The redshifts of these absorbers ($z < 0.15$) allow us to compare their locations with 1.07 million galaxy redshifts and positions from the CfA (2005 January) catalog, the SDSS (DR4), and the 2dF-FDR, 6dF-DR2, and Veron-11 catalogs. In regions where the galaxy surveys are complete to at least L^* , we found 23 O VI detections and 32 nondetections.

The major results of our study can be summarized as follows:

1. We confirm that stronger Ly α absorbers ($N_{\text{H I}} = 10^{13.2} - 10^{16.5} \text{ cm}^{-2}$) are 3 times closer to ($\geq 0.1L^*$) galaxies, on average, than weaker absorbers. Nearest neighbor statistics suggest that these absorbers are related to galaxy supercluster filaments.
2. Among the stronger Ly α lines, we found 10 Ly α absorbers in voids ($\sim 15\%$ of the total), with nearest neighbor galaxies more than $3 h_{70}^{-1}$ Mpc away. Interestingly, none of these void absorbers were detected in O VI.
3. The O VI and C III absorbers nearly always lie within $800 h_{70}^{-1}$ kpc of galaxies in L^* -complete regions. Nearest neighbor statistics place these absorbers sufficiently close to individual galaxies that they could be associated with winds or halos. Correcting for covering factors, we estimate that metals have been spread to median distances $350 - 500 h_{70}^{-1}$ kpc from L^* galaxies and $200 - 270 h_{70}^{-1}$ kpc from $0.1L^*$ galaxies.
4. A substantial percentage ($16/37 = 43\%$) of O VI absorbers are associated with Ly α absorption in close pairs with $(\Delta v)_{\text{Ly}\alpha} = 50 - 200 \text{ km s}^{-1}$. This velocity difference suggests a physical origin of some O VI absorbers in shock-heated gas.

We now elaborate on these overall conclusions and their implications. In general, the median distance between any two $\geq 0.1L^*$ galaxies is less than the median distance from the absorbers to the nearest $\geq 0.1L^*$ galaxy (Table 1, col. [5]). Thus, it is often difficult to determine which galaxy, if any, is the source of the gas in the absorber, a result consistent with numerical simulations (Davé et al. 1999). A more sensible picture places the Ly α absorbers within supercluster filaments. The nearest neighbor statistics for both O VI and C III absorbers place them sufficiently close to individual galaxies that some could be associated with winds or halos. Because few absorber regions have been surveyed below $0.1L^*$, we cannot exclude the possibility that metal line absorbers are associated with undiscovered faint galaxies. Some very faint galaxies have been found close to individual metal line absorbers (Table 2; van Gorkom et al. 1996; Shull et al. 1996; Stocke et al. 2006), suggesting that dwarf galaxy superwinds could be responsible for many weak metal line systems. New galaxy survey work around the very nearest ($cz \leq 5000 \text{ km s}^{-1}$) absorbers is underway to test this possibility.

The O VI and C III detections correspond to $\geq 10\%$ of solar metallicity for plausible models of collisional ionization and photoionization, respectively. The statistics of this sample suggest that metals have been spread to median distances of $350 - 500 h_{70}^{-1}$ kpc from L^* galaxies and $200 - 270 h_{70}^{-1}$ kpc from $0.1L^*$ galaxies, regardless of whether these galaxies are the source of these metals. The quoted range reflects the presence of regions of uncertain metallicity when the Ly α absorption is weak or undetected. The extent of metal transport must be variable, since C III and O VI detections and nondetections are found at comparable distances from galaxies. Weak Ly α ($N_{\text{H I}} < 10^{13.2} \text{ cm}^{-2}$) detections and nondetections are present in our sample with similar nearest neighbor distances, but we do not know their metallicity.

The O VI absorbers associated with close pairs of Ly α with $(\Delta v)_{\text{Ly}\alpha} = 50 - 200 \text{ km s}^{-1}$ imply velocities in the correct range to produce large amounts of O VI in shocks (Shull et al. 2003; Tumlinson et al. 2005). About half of all O VI absorbers, as well as half the O VI absorbers in Ly α line pairs, are found in or near groups of galaxies. In the Ly α absorber complex toward PKS 2155-304 (Shull et al. 1998, 2003), some of the absorbers contain O VI in apparent association with galaxy groups. Dwarf galaxies with $\sim 100 h_{70}^{-1}$ kpc halos or winds will have that gas stripped by frequent collisions with other dwarfs in $\lesssim 10^9$ yr. For the O VI absorbers in or near galaxy groups, a nearby dwarf may not be present, having been stripped of its gas to make a more general intragroup medium, as envisioned originally by Mulchaey et al. (1996).

The O VI/Ly α pairs are found closer to galaxies, by about a factor of 2 compared to the overall O VI absorber sample from which they were chosen. The median distance between any one of these absorbers and a galaxy of *any* luminosity in L^* -complete regions is $190 h_{70}^{-1}$ kpc, from which we extrapolate that most of these O VI absorbers are $\leq 100 h_{70}^{-1}$ kpc from galaxies at $0.1L^*$ or fainter. These nearest galaxy distances are a close match to galaxy distances from collisionally ionized WHIM in the Davé et al. (1999) simulations. Given their relationship to other nearby absorbers and to nearby galaxies, we interpret the O VI/Ly α line pairs as shocked, collisionally ionized gas. This type of O VI absorber shares some observational similarities with Galactic HVCs (Sembach et al. 2003; Collins et al. 2005; Fox et al. 2005). The O VI sample in Ly α pairs is substantial, with five pairs per unit redshift at low z . These O VI absorptions are sufficient to account for most or all of the excess power seen in the TPCF of Ly α absorbers (Paper IV).

Guided by the maximum extent to which metals are spread from galaxies, we define a filament-absorber association for systems $\leq 800 h_{70}^{-1}$ kpc from the nearest galaxy, in regions surveyed down to at least L^* . Because filaments are typically $5 - 7 h_{70}^{-1}$ Mpc across (Ramella et al. 1992), the nearest galaxy usually lies well within the filament. Our estimate of $800 h_{70}^{-1}$ kpc is a reasonable choice, given the average density of galaxies within a filament. From our results of § 3.3, we envision an empirical model for a supercluster filament in the local universe, composed of three generic regions: (1) region 1 (33%–50% coverage) composed of metal-enriched ($[Z] \gtrsim -1$) absorbers, (2) region 2 (16%–25% coverage) of low-metallicity absorbers, and (3) region 3 (25%–50% coverage) of unknown metallicity, owing to weak detections or nondetections of Ly α .

Our previous work led us to conclude that weaker Ly α absorbers are only loosely associated with galaxies (see Fig. 1) and may represent a population of uniformly distributed absorbers (Paper III). We propose here that the weaker Ly α absorbers lie in regions of low metallicity and should be added to the accounting of region 2. In 10^6 K gas, with neutral fraction $f_{\text{H I}} \approx 10^{-6}$, the

WHIM produces broad, shallow Ly α absorption. Therefore, the Ly α nondetections might be metal-rich regions too hot to be seen in Ly α absorption, but visible in *Chandra* spectra of high-ionization metal-line absorptions (Fang et al. 2002; Nicastro et al. 2005). The extent of metal transport calculated above refers to the spread of gas of 0.1 Z_{\odot} metallicity from galaxies in the current epoch. Absorbers more than $1 h_{70}^{-1}$ Mpc from galaxies may all contain gas at $[Z] \approx -1.5$ in the current epoch or they may be metal-free. We do not address the presence or absence of very metal-poor gas (e.g., absorbers of 3% solar metallicity at high z ; Aguirre et al. 2002).

The authors acknowledge several *HST* and *FUSE* grants to the University of Colorado in support of this work: HST-GO-06593.01, GO-08182.01, AR-09221.01, FUSE NNG04GA18G,

the *HST/COS* project (NAS5-98043), NASA NAG5-7262, NSF AST 02-06042, and FUSE NAG5-13004. J. T. acknowledges partial support from the Department of Astronomy and Astrophysics at the University of Chicago and HST-G0-9874.01-A. We thank John Huchra and Nathalie Martimbeau for providing timely updates to the CfA Redshift Survey Catalog, R. J. Weymann for his assistance with galaxy survey work, and Mark Giroux for comments on the manuscript. This work was based partially on observations obtained with the Apache Point Observatory 3.5 m telescope, which is owned and operated by the Astrophysical Research Consortium. Funding for the creation and distribution of the SDSS Archive (<http://www.sdss.org>) has been provided by the Alfred P. Sloan Foundation, the Participating Institutions, NASA, NSF, the US Department of Energy, the Japanese Monbukagakusho, and the Max Planck Society.

REFERENCES

- Abazajian, K., et al. 2003, *AJ*, 126, 2081
 ———. 2004, *AJ*, 128, 502
 Aguirre, A., Schaye, J., & Theuns, T. 2002, *ApJ*, 576, 1
 Aracil, B., Petitjean, P., Smette, A., Surdej, J., Mückel, J. P., & Cristiani, S. 2002, *A&A*, 391, 1
 Blanton, M. R., et al. 2003, *ApJ*, 592, 819
 Cen, R., & Ostriker, J. P. 1999, *ApJ*, 517, 31
 Chen, H.-W., Lanzetta, K. M., & Fernandez-Soto, A. 2000, *ApJ*, 533, 120
 Chen, H.-W., Lanzetta, K. M., Webb, J. L., & Barcons, X. 1998, *ApJ*, 498, 77
 Chen, H.-W., Prochaska, J. X., Weiner, B. J., Mulchaey, J. S., & Williger, G. M. 2005, *ApJ*, 629, L25
 Colless, M., et al. 2001, *MNRAS*, 328, 1039
 ———. 2003, The 2dF Galaxy Redshift Survey
 Collins, J. A., Shull, J. M., & Giroux, M. L. 2004, *ApJ*, 605, 216
 ———. 2005, *ApJ*, 623, 196
 Danforth, C. W., & Shull, J. M. 2005, *ApJ*, 624, 555 (DS05)
 Danforth, C. W., Shull, J. M., Rosenberg, J. L., & Stocke, J. T. 2006, *ApJ*, 640, 716
 Davé, R., Hernquist, L., Katz, N., & Weinberg, D. 1999, *ApJ*, 511, 521
 Davé, R., et al. 2001, *ApJ*, 552, 473
 Drozdovsky, I. O., Schulte-Ladbeck, R. E., Hopp, U., Crone, M. M., & Greggio, L. 2001, *ApJ*, 551, L135
 Fang, T., et al. 2002, *ApJ*, 572, L127
 Fox, A. J., Wakker, B. P., Savage, B. D., Tripp, T. M., Sembach, K. R., & Bland-Hawthorn, J. 2005, *ApJ*, 630, 332
 Hoyle, F., Rojas, R. R., Vogeley, M., & Brinkmann, J. 2005, *ApJ*, 620, 618
 Huchra, J., Geller, M., & Corwin, H. 1995, *ApJS*, 99, 391
 Huchra, J., Geller, M., de Lapparent, V., & Corwin, H. 1990, *ApJS*, 72, 433
 Huchra, J., Vogeley, M., & Geller, M. 1999, *ApJS*, 121, 287
 Impey, C. D., Petry, C. E., & Flint, K. P. 1999, *ApJ*, 524, 536
 Indebetouw, R., & Shull, J. M. 2004, *ApJ*, 605, 205
 Jones, D. H., Saunders, W., Read, M., & Colless, M. 2005, *Publ. Astron. Soc. Australia*, 22, 277
 Lanzetta, K. M., Bowen, D. V., Tytler, D., & Webb, J. K. 1995, *ApJ*, 442, 538
 Martin, C. L. 2003, in *The IGM/Galaxy Connection*, ed. J. Rosenberg & M. Putman (Dordrecht: Kluwer), 205
 Marzke, R. O., da Costa, L. N., Pellegrini, P. S., Willmer, C. N. A., & Geller, M. J. 1998, *ApJ*, 503, 617
 McLin, K. M. 2002, Ph.D. thesis, Univ. Colorado
 McLin, K. M., Stocke, J. T., Weymann, R. J., Penton, S. V., & Shull, J. M. 2002, *ApJ*, 574, L115
 Morris, S. L., Weymann, R. J., Dressler, A., McCarthy, P. J., Smith, B. A., Terrile, R. J., Giovanelli, R., & Irwin, M. 1993, *ApJ*, 419, 524
 Mulchaey, J. S., Mushotzky, R. F., Burstein, D., & Davis, D. S. 1996, *ApJ*, 456, L5
 Nicastro, F., et al. 2005, *Nature*, 433, 495
 Oke, J. B., & Sandage, A. 1968, *ApJ*, 154, 21
 Park, C., et al. 2005, *ApJ*, 633, 11
 Penton, S. V., Shull, J. M., & Stocke, J. T. 2000a, *ApJ*, 544, 150 (Paper II)
 Penton, S. V., Stocke, J. T., & Shull, J. M. 2000b, *ApJS*, 130, 121 (Paper I)
 ———. 2002, *ApJ*, 565, 720 (Paper III)
 ———. 2004, *ApJS*, 152, 29 (Paper IV)
 Prochaska, J. X., Chen, H.-W., Howk, J. C., Weiner, B. J., & Mulchaey, J. S. 2004, *ApJ*, 617, 718
 Ramella, M., Geller, M. J., & Huchra, J. P. 1992, *ApJ*, 384, 396
 Savage, B. D., Lerner, N., Wakker, B. P., Sembach, K. R., & Tripp, T. M. 2005, *ApJ*, 626, 776
 Savage, B. D., Sembach, K. R., Tripp, T. M., & Richter, P. 2002, *ApJ*, 564, 631
 Sembach, K. R., Savage, B. D., Lu, L., & Murphy, E. M. 1999, *ApJ*, 515, 108
 Sembach, K. R., et al. 2003, *ApJS*, 146, 165
 Shull, J. M. 2002, in *ASP Conf. Ser. 254, Extragalactic Gas at Low Redshift*, ed. J. S. Mulchaey & J. T. Stocke (San Francisco: ASP), 51
 Shull, J. M., & McKee, C. F. 1979, *ApJ*, 227, 131
 Shull, J. M., Penton, S. V., Stocke, J. T., Giroux, M. L., van Gorkom, J. H., Lee, Y. H., & Carilli, C. 1998, *AJ*, 116, 2094
 Shull, J. M., Stocke, J. T., & Penton, S. V. 1996, *AJ*, 111, 72
 Shull, J. M., Tumlinson, J., & Giroux, M. L. 2003, *ApJ*, 594, L107
 Slezak, E., de Lapparent, V., & Bijou, A. 1993, *ApJ*, 409, 517
 Stocke, J. T., Keeney, B. A., McLin, K. M., Rosenberg, J. L., Weymann, R. J., & Giroux, M. L. 2004, *ApJ*, 609, 94
 Stocke, J. T., Shull, J. M., & Penton, S. V. 2006, in *Planets to Cosmology*, ed. S. Casertano & M. Livio (Cambridge: Cambridge Univ. Press), in press (astro-ph/0407352)
 Stoughton, C., et al. 2002, *AJ*, 123, 485
 Strauss, M. A., et al. 2002, *AJ*, 124, 1810
 Sutherland, R. S., & Dopita, M. A. 1993, *ApJS*, 88, 253
 Szomoru, A., Guhathakarta, P., van Gorkom, J. H., Knapen, J. H., Weiberg, D. H., & Fruchter, A. S. 1994, *AJ*, 108, 491
 Tripp, T. M., Bowen, D. V., Sembach, K. R., Jenkins, E. B., Savage, B. D., & Richter, P. 2006, in *ASP Conf. Ser. 348, Astrophysics in the Far Ultraviolet: Five Years of Discovery with FUSE*, ed. G. Sonneborn, H. W. Moos, & B.-G. Andersson (San Francisco: ASP), in press (astro-ph/0411151)
 Tripp, T. M., Giroux, M. L., Stocke, J. T., Tumlinson, J., & Oegerle, W. R. 2001, *ApJ*, 563, 724
 Tripp, T. M., Lu, L., & Savage, B. D. 1998, *ApJ*, 508, 200
 Tripp, T. M., Savage, B. D., & Jenkins, E. B. 2000, *ApJ*, 534, L1
 Tripp, T. M., et al. 2002, *ApJ*, 575, 697
 Tumlinson, J., & Fang, T. 2005, *ApJ*, 623, L97
 Tumlinson, J., Shull, J. M., Giroux, M. L., & Stocke, J. T. 2005, *ApJ*, 620, 95
 van Gorkom, J. H., Carilli, C. L., Stocke, J. H., Perlman, E. J., & Shull, J. M. 1996, *AJ*, 112, 1397
 Veron-Cetty, M. P., & Veron, P. 2003, *A&A*, 412, 399
 Viel, M., Branchini, E., Cen, R., Ostriker, J. P., Matarrese, S., Mazzotta, P., & Tully, B. 2005, *MNRAS*, 360, 1110
 Vogeley, M. S., Geller, M. J., & Huchra, J. P. 1991, *ApJ*, 382, 44